JGR Oceans

RESEARCH ARTICLE
10.1029/2024JC021414

Special Collection:
Physical and biogeochemical processes affecting nutrients and the carbon cycle in mesoscale eddies of subtropical oceans

Elevated Heterotrophic Prokaryotic Production Supported by Low Nucleic Acid Prokaryotes at a Cyclonic Eddy Edge in the Northwest Pacific

Junyi Ni[1], Mingming Chen[1], Jiaming Shen[1], Li Liu[1], Zong-Pei Jiang[2], Kuanbo Zhou[1], Xiaolin Li[1], Minhan Dai[1], and Yao Zhang[1]

[1]State Key Laboratory of Marine Environmental Science and College of Ocean and Earth Sciences, Xiamen University, Xiamen, China, [2]Ocean College, Zhejiang University, Zhoushan, China

Abstract The cyclonic eddy uplifts nutrient-rich seawater into the euphotic zone, typically directly enhancing phytoplankton abundance and primary production. However, its impact on heterotrophic prokaryotic production (HPP) remains unclear due to the complex interplay of multiple indirect factors governing this process. Here, we conducted a comprehensive investigation of the distribution of picophytoplankton and heterotrophic prokaryotes, prokaryotic community structure, and HPP within a cyclonic eddy in the western North Pacific subtropical gyre. The results indicated that despite the higher abundance of picophytoplankton accompanied by nutrient upwelling at the eddy core compared to the edge, higher levels of HPP were observed at the eddy edge between 100 and 200 m, consistent with the distribution of the low nucleic acid content (LNA) prokaryotes. The significant positive correlation between HPP and the proportion of LNA group in total heterotrophic prokaryotes suggested a primary contribution from the LNA group over the high nucleic acid content (HNA) group. SAR11, a typical member of the LNA group, may primarily contribute to the elevated HPP observed at the eddy edge. The changes in temperature, nutrients, and light intensity induced by the cyclonic eddy may significantly influence the distribution and activity of HNA and LNA groups, potentially exerting a greater impact on HPP compared to phytoplankton-related factors. These findings contribute to understanding the underlying mechanisms of HPP responses to cyclonic eddies in the oligotrophic open ocean.

Plain Language Summary Mesoscale eddies are common features of global ocean circulation. Cyclonic eddies uplift isopycnals at their centers, bringing cold, nutrient-rich waters from the lower layers to the surface within the eddy, thereby promoting higher phytoplanktonic abundance and primary production typically observed at the eddy core. However, the response of heterotrophic prokaryotic distribution and heterotrophic prokaryotic production (HPP) to the upwelling in the cyclonic eddy remains unclear, as limited studies have not yet reached a consensus. We tracked a cyclonic eddy in the western North Pacific subtropical gyre to compare prokaryotic abundance, community composition, and HPP between eddy core and edge. The results indicate that, while picophytoplankton abundance was higher at the eddy core compared to the edge, HPP was predominantly elevated at the edge in response to the cyclonic eddy. The low nucleic acid content (LNA) prokaryotes dominated by SAR11 may significantly contribute to the increased HPP, as opposed to the traditionally assumed high nucleic acid content (HNA) group. The main factors influencing the distribution of LNA and HNA groups, as well as HPP, include temperature, nutrients, and light intensity altered by the eddy. This study advances the understanding of heterotrophic prokaryotic responses to cyclonic eddy dynamics.

Key Points:

- Higher heterotrophic prokaryotic production (HPP) occurred at the eddy edge, while picophytoplankton predominantly occurred in the core
- The elevated HPP at the eddy edge was attributed to low nucleic acid prokaryotes, such as SAR11
- The altered temperature, nutrients, and light intensity may impact the distribution and HPP in the eddy

Supporting Information:

Supporting Information may be found in the online version of this article.

Correspondence to:

Y. Zhang,
yaozhang@xmu.edu.cn

Citation:

Ni, J., Chen, M., Shen, J., Liu, L., Jiang, Z.-P., Zhou, K., et al. (2024). Elevated heterotrophic prokaryotic production supported by low nucleic acid prokaryotes at a cyclonic eddy edge in the Northwest Pacific. *Journal of Geophysical Research: Oceans*, *129*, e2024JC021414. https://doi.org/10.1029/2024JC021414

Received 2 JUN 2024
Accepted 10 NOV 2024

Author Contributions:

Conceptualization: Yao Zhang
Data curation: Minhan Dai, Yao Zhang
Formal analysis: Junyi Ni
Funding acquisition: Minhan Dai, Yao Zhang
Investigation: Junyi Ni, Mingming Chen, Jiaming Shen, Li Liu, Zong-Pei Jiang, Kuanbo Zhou, Xiaolin Li
Project administration: Minhan Dai, Yao Zhang

1. Introduction

Mesoscale eddies (10–100 km) are widely distributed in the upper layers of the ocean (Chelton et al., 2011). Within cyclonic eddies, cold, nutrient-rich, deep seawater was lifted to the euphotic zone, influencing the biogeochemical cycles in the upper ocean. It has been widely reported that the upwelling of nutrients stimulates the growth of phytoplankton, thereby increasing primary production (Falkowski et al., 1991; Hu et al., 2014; Rii et al., 2008; Singh et al., 2015). The increase in phytoplankton abundance and primary production would lead to an elevated release of dissolved organic carbon (DOC), which could potentially stimulate heterotrophic prokaryotic growth (Brown et al., 2008). Consequently, there may be an increase in the abundance and biomass production (i.e., commonly referred to as heterotrophic prokaryotic production (HPP)). Nevertheless, studies have shown that the peak values of HPP, as well as the highest abundances of heterotrophic prokaryotes and phytoplankton, did not consistently occur in the same regions within cyclonic eddies (Devresse et al., 2022;

Resources: Minhan Dai, Yao Zhang
Supervision: Minhan Dai, Yao Zhang
Validation: Junyi Ni
Visualization: Junyi Ni
Writing – original draft: Junyi Ni
Writing – review & editing: Junyi Ni, Mingming Chen, Jiaming Shen, Li Liu, Zong-Pei Jiang, Kuanbo Zhou, Xiaolin Li, Minhan Dai, Yao Zhang

Fourquez et al., 2021). Variations in environmental and biological factors, such as temperature, nutrients, and viruses (Albright, 1975; Cruz & Neuer, 2019; Gasol et al., 2009; Mojica et al., 2020; Pomeroy & Wiebe, 2001; Rowe et al., 2012; Ruiz-González et al., 2012), can influence the composition and activity of heterotrophic prokaryotes, thereby impacting the distribution of HPP within cyclonic eddies.

Heterotrophic prokaryotes include high nucleic acid content (HNA) and low nucleic acid content (LNA) groups (Gasol et al., 1999). HNA cells exhibit larger genome sizes and cell volumes, whereas LNA cells exhibit the opposite. At first, HNA groups were thought to be primarily active contributors to HPP, while LNA cells were considered as potential dormant or dead cells (Gasol et al., 1999; Lebaron et al., 2001). Recent studies have challenged this theory. For example, in the oligotrophic Mediterranean Sea, an unexpected negative correlation was found between HPP and the proportion of HNA groups in total heterotrophic prokaryotes (Van Wambeke et al., 2011). Growing evidence has revealed that considerable heterotrophic activity of LNA groups is comparable to that of HNA groups, significantly contributing to HPP in the ocean (Longnecker et al., 2005; Scharek & Latasa, 2007; Zubkov et al., 2001). Within the LNA groups, SAR11 is a typical oligotroph with a small and streamlined genome; this genomic trait reduces cell division costs and enhances their adaptation to oligotrophic environments compared to microbes with larger genomes (Giovannoni, 2017; Giovannoni et al., 2005; Mary et al., 2006). In contrast, most members of the HNA group (such as Bacteroidetes and Rhodobacterales) are considered copiotrophs (Schattenhofer et al., 2011; Vila-Costa et al., 2012). Generally, oligotrophs thrive in stable conditions, whereas copiotrophs dominate when turbulence causes fluctuations in nutrient availability (Bentkowski et al., 2015; Giovannoni, 2017; Vila-Costa et al., 2019).

The cyclonic eddy core receives nutrient replenishment through upwelling in the oligotrophic ocean. However, there is limited knowledge regarding whether HPP in these eddies is predominantly driven by HNA or LNA groups and the connection between HPP and the compositions of these two groups. To date, only two related studies have been carried out in the North Atlantic and the sub-Antarctic region of the Southern Ocean, with analysis conducted at only 2–3 sampling stations within cyclonic eddies (Fourquez et al., 2021; Mojica et al., 2020). The outcomes of the two studies yielded contrasting results. In the North Atlantic study, a positive correlation was observed between the percentage of HNA cells and HPP (Mojica et al., 2020), while a negative correlation was discovered in the Southern Ocean (Fourquez et al., 2021). The western North Pacific subtropical gyre (wNPSG) is one of the most oligotrophic regions globally (Dore et al., 2008; Karl, 1999; Robidart et al., 2019), known for its frequent eddy activities (Qiu et al., 2014). Picophytoplankton, including *Prochlorococcus*, *Synechococcus*, and picoeukaryotes (Raven, 1998), are the dominant primary producers, accounting for 68%–83% of the primary production in the NPSG (Li et al., 2011; Rii et al., 2016; Wei et al., 2021). It remains unknown how these picophytoplankton, the heterotrophic HNA and LNA groups, and the HPP driven by the HNA and LNA groups respond to mesoscale cyclonic eddies in the wNPSG. Here, we conducted high spatial resolution surveys within a cyclonic eddy of the wNPSG with the aim of (a) clarifying the distribution of picophytoplankton, HNA and LNA groups, and HPP, (b) revealing the connection between HPP and the compositions of HNA and LNA groups, and (c) elucidating potential factors influencing the HPP in the cyclonic eddy system.

2. Materials and Methods

2.1. Sampling and Biogeochemical Parameters

The cruise was conducted aboard the R/V *TAN KAH KEE* from 15 March to 20 April 2019, in the wNPSG. A cyclonic eddy was tracked by monitoring the daily average sea level anomaly (SLA) data obtained from the Copernicus Climate Data Store (https://cds.climate.copernicus.eu/). The eddy core and edges were identified using the SLA and real-time horizontal velocity derived from the onboard acoustic Doppler current profiler (WH300 kHz, Teledyne RD Instruments). Samples were collected at 19 stations, with depth profiles ranging from 0 to 500 m, along the four transects crossing the cyclonic eddy (Figure 1). Temperature, salinity, density, and fluorescence (mainly from chlorophyll) were measured using a conductivity-temperature-depth (CTD, Sea-Bird SBE911 plus) profiler. Ammonium concentration was measured on board using the fluorometric *o*-phthaldialdehyde method with a detection limit of 1.3 nmol L^{-1} (Zhu et al., 2013). Nitrite (NO_2^-) and nitrate (NO_3^-) concentrations were determined in the laboratory using classical colorimetric methods with a Technicon AutoAnalyzer III (AA3, Brand + luebbe). The detection limits were NO_2^- > 5 nmol L^{-1} and NO_3^- > 70 nmol L^{-1}

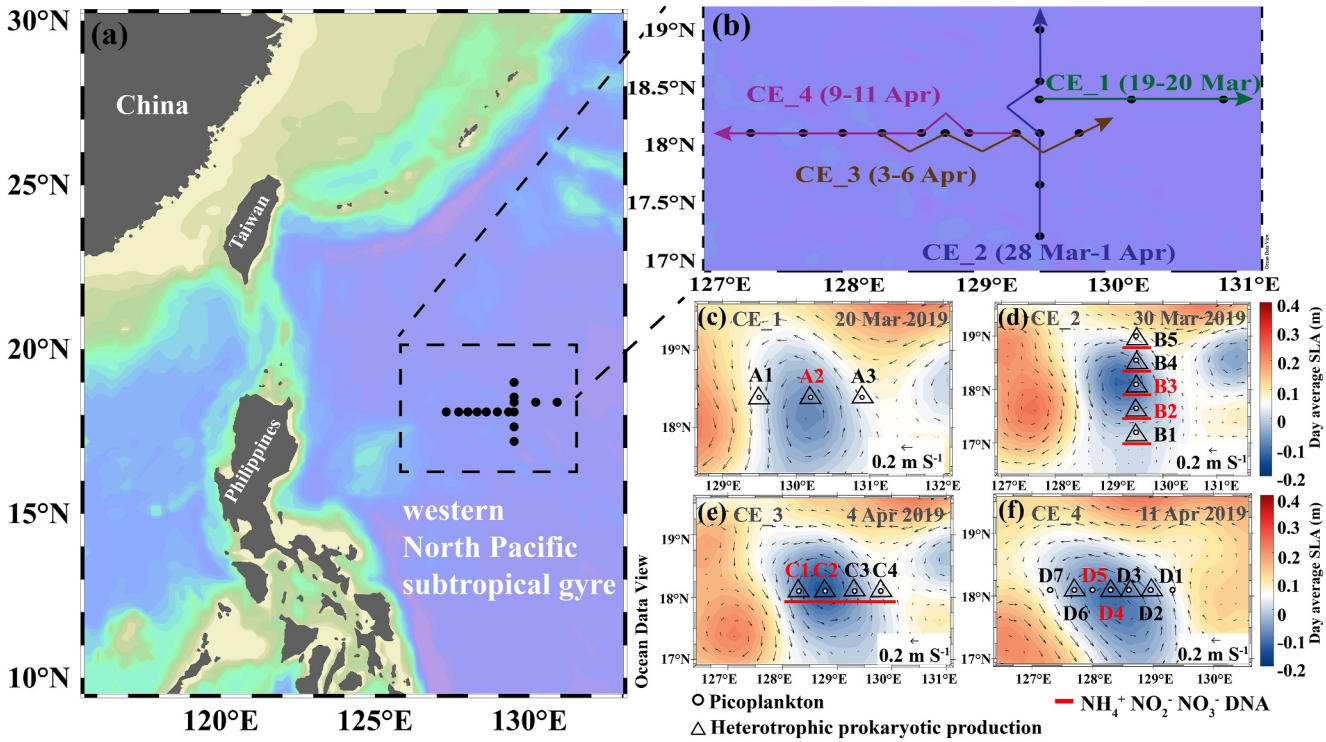

Figure 1. Study area, sampling stations, and the distribution of sea level anomaly (SLA). (a) Study area; (b) Sampling transects; (c–f) Sampling stations in the background of the SLA map with roughly corresponding sampling times. Gray arrows show satellite-derived surface current velocities. SLA and surface current velocities were obtained from the Copernicus Climate Data Store (https://cds.climate.copernicus.eu/). The stations labeled in red and black indicate the eddy core and edge, respectively.

(Dai et al., 2008; Zhang, 2000). The detailed nutrient analysis methods and data have been published in Liu et al. (2023).

2.2. Picoplankton Abundance and Biomass

The collected seawater was pre-filtered through a 20 μm pore size nylon mesh filter to remove large-sized plankton. 2 mL of pre-filtered seawater was fixed with glutaraldehyde (final concentration 0.5%; Aladdin) for 15 min in the dark at room temperature. Then, the samples were flash-frozen using liquid nitrogen and stored at −80°C until examination in the laboratory. *Prochlorococcus*, *Synechococcus*, and picoeukaryotes were identified and counted using the FACSAria flow cytometer (Figure S1a in Supporting Information S1) (Becton, Dickinson, and Company) (Olson et al., 1990). Their carbon biomass was estimated based on the single-cell carbon content obtained from literature (Table S1 in Supporting Information S1), which indicates that *Prochlorococcus*, *Synechococcus*, and picoeukaryotes have single-cell carbon content of 44, 126, and 264 fg cell^{-1}, respectively. Heterotrophic prokaryotes were identified and quantified after staining with SYBR-Green I (final concentration of 0.01%; Invitrogen) (Marie et al., 1997). Heterotrophic HNA and LNA groups were differentiated based on the green fluorescence intensity corresponding to their nucleic acid content (Figure S1b and S1c in Supporting Information S1) (Gasol et al., 1999). When the fluorescence signals of picophytoplankton and HNA cells overlapped, the abundance of the HNA group was determined by subtracting the abundance of picophytoplankton from the total number of cells showing intense green fluorescence.

2.3. Heterotrophic Prokaryotic Production

The collected seawater was divided into five 2 mL sterile centrifuge tubes, with three replicates in the experimental group and two in the control group. ^{3}H-leucine solution (final concentration of 20 nmol L^{-1}; Perkin Elmer) was added to 1.5 mL of seawater sample in each tube. Immediately, a trichloroacetic acid solution pre-cooled to 4°C (final concentration of 5%; Sigma) was added to the control tubes to halt microbial activity. The samples were placed in a chamber at an in situ temperature for dark incubation for 1–2 hr for samples above 200 m, and 10–24 hr

for samples below 200 m (Nagata et al., 2000). The 4°C pre-cooled trichloroacetic acid solution (final concentration of 5%; Sigma) was added to terminate the incubation. The samples were frozen at −80°C until analysis. In the laboratory, the samples were processed following the micro-centrifugation technique (Kirchman et al., 1985) and then added with 0.5 mL of scintillation cocktail (Perkin Elmer). The samples were counted using a Tri-Carb 2800TR liquid scintillation counter (Perkin Elmer). ^{3}H-leucine uptake was converted to carbon units by applying a conversion factor of 0.37 kg C mol^{-1} leucine (Huang et al., 2019).

2.4. Prokaryotic Community Composition

The seawater samples (2 L) were filtered using a 0.2 μm pore size polycarbonate membrane (45 mm diameter; Millipore) within one hour. The filters were flash-frozen in liquid nitrogen and stored at −80°C. DNA extraction was performed using the Powerwater DNA Isolation Kit (MoBio Laboratories) following the manufacturer's protocol. The V4 hypervariable region of the 16S rRNA gene was PCR-amplified using universal primers 515F (GTGYCAGCMGCCGCGGTAA) and 806R (GGACTACNVGGGTWTCTAAT) (Apprill et al., 2015; Parada et al., 2016). The PCR conditions were as follows: 3 min of initial denaturation at 95°C; followed by 35 cycles of denaturation at 95°C (30 s), annealing at 55°C (45 s), elongation at 72°C (45 s); and a final extension at 72°C for 10 min. The PCR product was used for library preparation, and the library was sequenced on an Illumina HiSeq2500 platform following the standard protocol at Huada Gene Institute (Shenzhen, China). The high-quality paired-end reads were merged into tags based on their overlaps using Fast Length Adjustment of Short reads (FLASH) (v1.2.11) (Magoč & Salzberg, 2011). The tags were clustered into Operational Taxonomic Units (OTUs) with a 97% similarity using UPARSE (v7.0.1090) (Edgar, 2013). Taxonomy was assigned using the Ribosomal Database Project (RDP) Classifier (v.2.2) (Cole et al., 2014) with the Greengenes database (DeSantis et al., 2006; McDonald et al., 2012) (https://greengenes.secondgenome.com/), employing a confidence threshold of 0.5.

2.5. Statistical Analyses

The significance of differences in picoplankton abundance, HPP, alpha diversity of the community, nutrient concentrations, temperature, and density between the eddy core and edge was assessed using either the Mann-Whitney *U* test or the Wilcoxon signed rank test. The correlations between picoplankton abundance/biomass, HPP, and biogeochemical parameters were analyzed using either Spearman's rank correlation or linear regression. Significant differences in community composition between the eddy core and edge were evaluated using ANOSIM. The relationship between community composition and environmental factors was explored through Canonical Correlation Analysis (CCA). The differences in the relative abundance of taxa between the eddy core and edge were examined using linear discriminant analysis effect size (LEfSe) method.

3. Results

3.1. Biogeochemical Background of Cyclonic Eddy

The SLA values in the core of the cyclonic eddy were more negative during the sampling of transects CE_1 to CE_4 than at other cruise times, indicating that the cyclonic eddy was in a mature stage during the sampling period (Figure S2 in Supporting Information S1). There were seven stations at the cyclonic eddy core and 12 stations at the edges (Figure 1). The eddy core stations featured lower temperatures and higher salinity and density than the edge stations at equivalent depths. The most pronounced temperature and density contrast between the eddy core and edge occurred within the depth range of 100–200 m (Figures S3a–S3d and S3i–S3l in Supporting Information S1). Nutrient-rich seawater can be uplifted into the euphotic zone, as indicated by the significantly higher integrated nitrate concentration within the euphotic zone (defined as 0.1% of photosynthetically available radiation, approximately 150 m here) at the eddy core compared to the edge ($P < 0.05$, Mann-Whitney *U* test; Figure S4 in Supporting Information S1), stimulating phytoplankton growth. Consequently, the maximum chlorophyll fluorescence value primarily occurred at the core stations (Figure S3m–S3p in Supporting Information S1).

3.2. Picophytoplankton Abundance and Carbon Biomass

The abundance maxima of *Prochlorococcus*, *Synechococcus*, and picoeukaryotes ($1.1 \pm 0.06 \times 10^{5}$, $3.3 \pm 0.2 \times 10^{3}$, and $4.8 \pm 0.2 \times 10^{3}$ cells mL^{-1}, respectively) all appeared at the eddy core stations. Their average

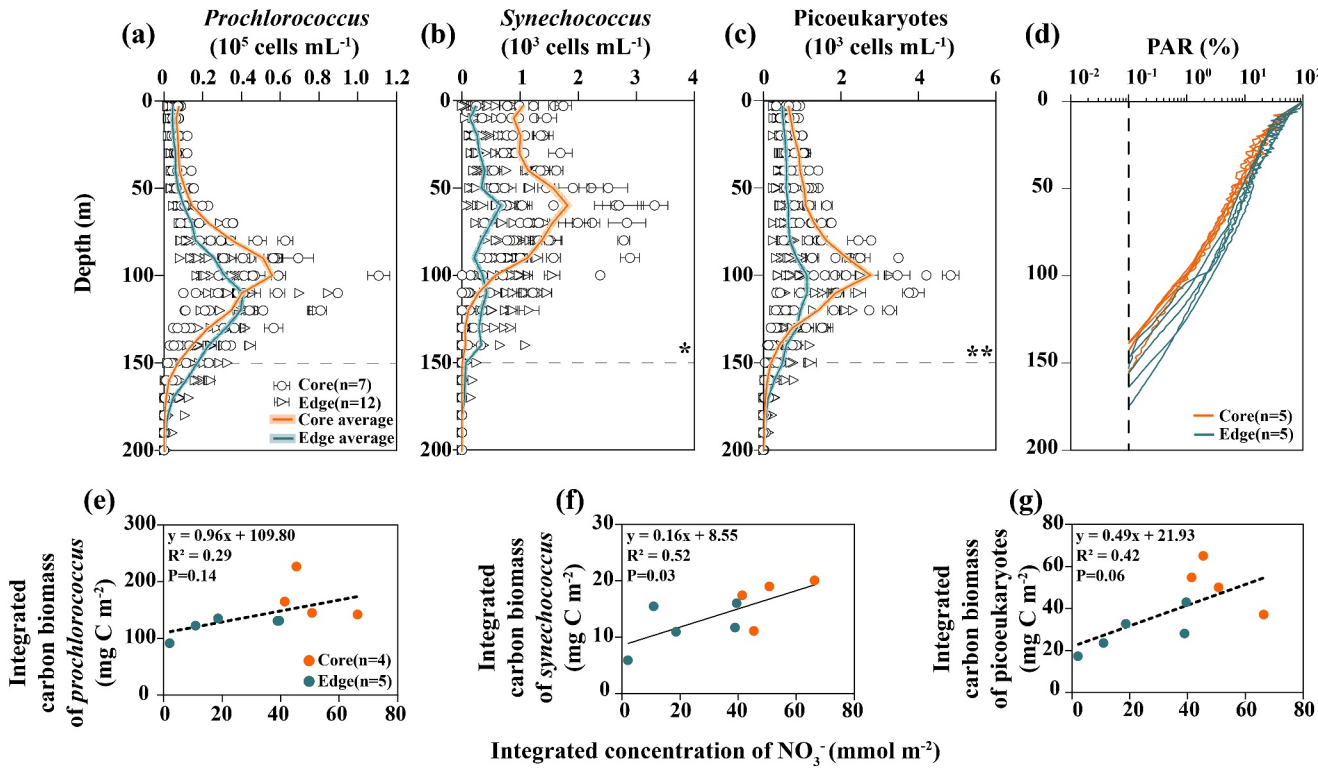

Figure 2. Distributions of picophytoplankton abundance and photosynthetically available radiation (PAR). (a) Depth profiles of *Prochlorococcus*, (b) *Synechococcus*, and (c) picoeukaryotes abundances. Gray dashed lines correspond to the average depth of the euphotic zone bottom (defined as 0.1% of the surface PAR). Asterisks denote a significant difference in the average abundance between the eddy core and edge within the euphotic zone (*$P < 0.05$; **$P < 0.01$, Wilcoxon signed rank test). Error bars represent the standard deviation (SD) of three technical replicates. Some error bars are not visible as they are smaller than the symbols. The shaded area indicates propagated error from the standard errors (SEs) of the average values. (d) Depth profile of relative PAR as a percentage of the surface PAR. (e) Linear regression analysis between the integrated carbon biomass of *Prochlorococcus*, (f) *Synechococcus*, and (g) picoeukaryotes and the integrated nitrate concentration for the upper 150 m. Error bars representing propagated error from the SEs are not visible as they are smaller than the symbols.

abundances at each depth of the eddy core stations and the edge stations indicated that there were shoaled depths of the abundance peaks of *Prochlorococcus* and picoeukaryotes at the eddy core compared to those at the edge (Figures 2a and 2c). Furthermore, *Synechococcus* and picoeukaryotes showed significantly higher abundances in the euphotic zone (Figure 2d) at the eddy core than at the edge (Wilcoxon signed rank test $P < 0.05$–0.01; Figures 2b and 2c). No significant difference was observed in the abundance of *Prochlorococcus* between the eddy core and the edge within the euphotic zone (Figure 2a). Based on the single-cell carbon content of *Prochlorococcus*, *Synechococcus*, and picoeukaryotes (Table S1 in Supporting Information S1), the carbon biomass of picophytoplankton increased by 44 mg C m^{-2} in the euphotic zone at the eddy core compared to the edge. The linear regression analysis between 150 m-integrated carbon biomass and nitrate concentration indicated that while *Synechococcus* had the lowest carbon biomass, it showed the most significant response to increased nitrate levels in the euphotic zone ($R^2 = 0.52$, $P < 0.05$) (Figures 2e–2g).

3.3. Heterotrophic Prokaryotic Abundance and Production

Displaying a similarity to picophytoplankton (especially *Synechococcus* and *Prochlorococcus*), heterotrophic prokaryotic abundance was higher above 100 m at the eddy core, while lower between 100 and 200 m at the eddy core compared to the edge ($P < 0.01$; Figure 3a). The LNA group exhibited a similar pattern to total heterotrophic prokaryotes (Figure 3b). The HNA group was more abundant at the eddy core above 100 m compared to the edge ($P < 0.01$), with no difference below 100 between the eddy core and edge (Figure 3c). The HNA group's contributions to the total heterotrophic prokaryotic abundance (HNA%) were significantly higher at the eddy core than at the edge across the water column above 200 m ($P < 0.05$; Figure 3d), while the LNA group's contributions to the total heterotrophic prokaryotic abundance (LNA%) were significantly higher at the eddy edge compared to the core above 200 m ($P < 0.05$; Figure 3e). Notably, the LNA group's abundance was predominant above 200 m

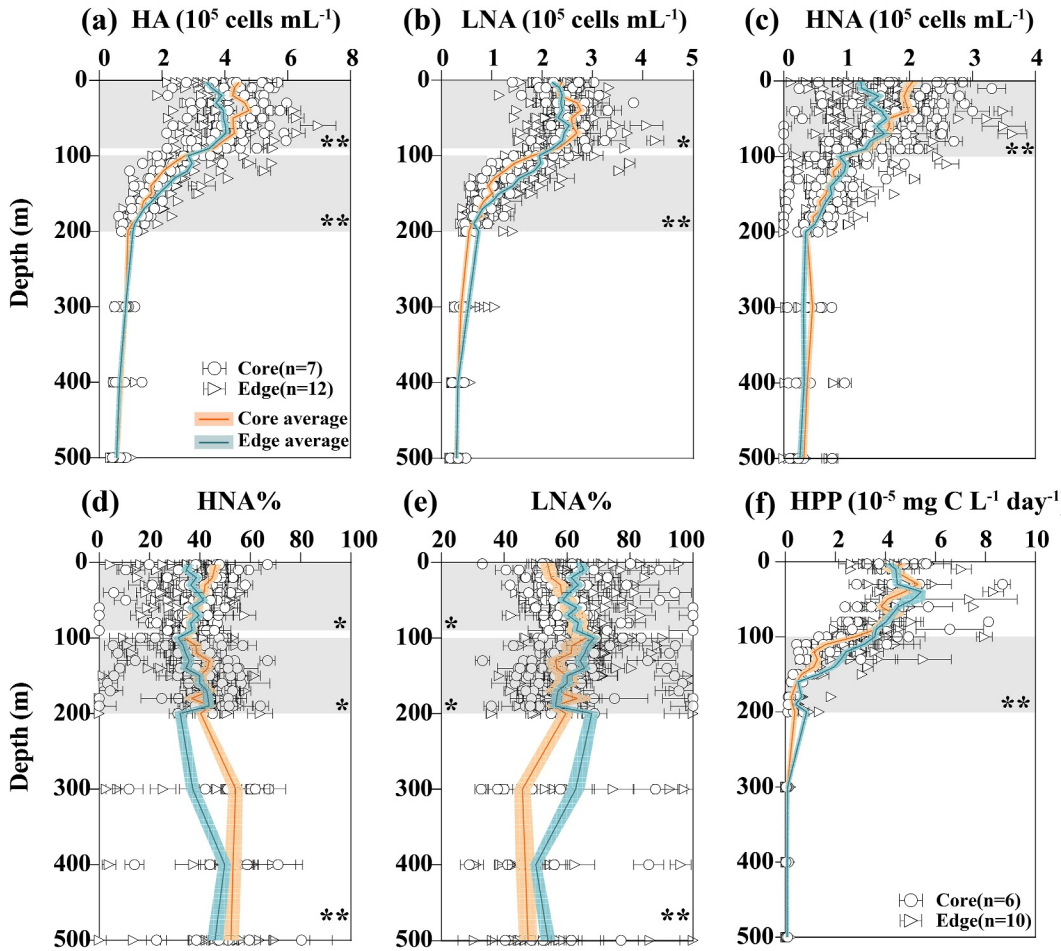

Figure 3. Distributions of heterotrophic prokaryotic abundance and production (HPP). (a) Depth profiles of abundances of heterotrophic prokaryotes (HA), (b) low nucleic acid (LNA) group, and (c) high nucleic acid (HNA) group. (d) Depth profiles of the proportions of HNA group (HNA%) and (e) LNA group (LNA%) in total heterotrophic prokaryotic abundance. (f) Depth profile of HPP. Error bars in (b) represent the standard deviation (SD) of three technical replicates; error bars in (a, c–e) represent propagated error from the standard errors (SEs) of three technical replicates; error bars in (f) represent the SD of three biological replicates. Some error bars are not visible as they are smaller than the symbols. The shaded area indicates the propagated error from the SEs of the average values. Gray background denotes a significant difference between the eddy core and edge for a given depth range (*$P < 0.05$; **$P < 0.01$, Wilcoxon signed rank test). Asterisks at the bottom of (d) and (e) indicate significant differences between the eddy core and edge in the water column above 500 m.

(54%–69%), both at the eddy core and at the edge. The HPP showed a significant difference, being higher at the eddy edge than at the core ($P < 0.01$; Figure 3f), only between 100 and 200 m, where the LNA group's abundance demonstrated a similar trend.

3.4. Prokaryotic Community Structure and Diversity

A total of 81 samples from 20 to 500 m were subjected to 16S rRNA gene amplicon sequencing. The number of high-quality reads ranged from 36,976 to 61,255 across the samples. The data set was standardized by randomly subsampling the read data from each sample to the lowest number of reads encountered for a sample. After subsampling, the reads were clustered into a total of 3,298 OTUs with 3,092 OTUs containing more than one read. The Good's coverage of the sample ranged from 0.990 to 0.997, indicating comprehensive coverage of species. The Chao1 diversity index, reflecting OTU richness, was higher at the eddy core than the edge between 20 and 200 m depths ($P < 0.05$, Wilcoxon signed rank test; Figure S5a in Supporting Information S1). The Shannon diversity index, representing both OTU richness and evenness, showed no significant difference between the eddy core and the edge (Figure S5b in Supporting Information S1). Canonical correlation analysis showed that the

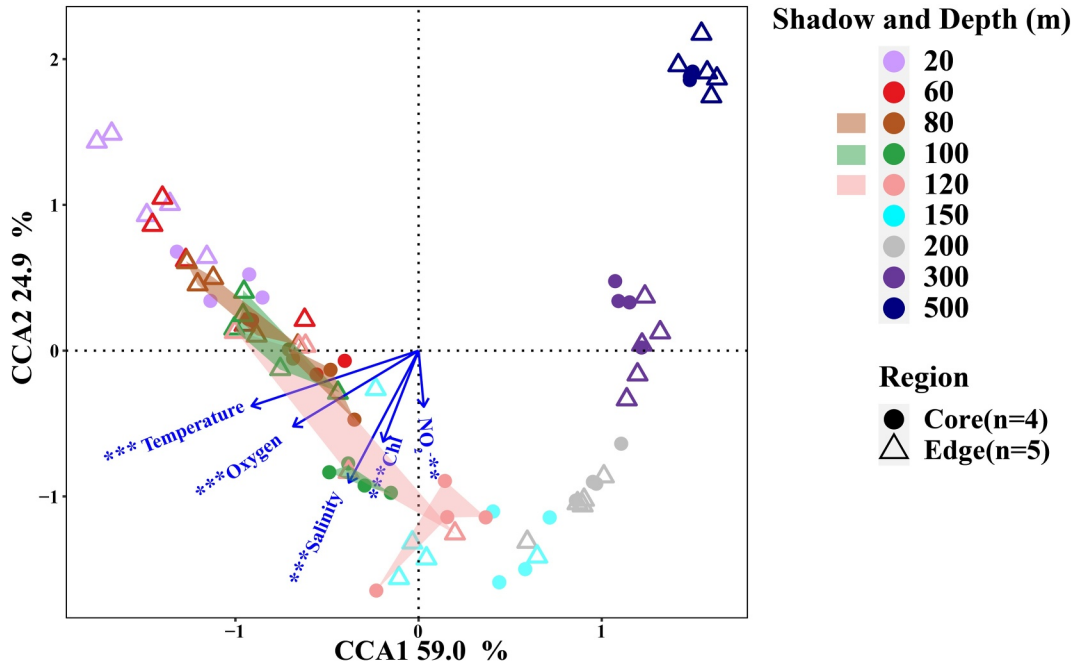

Figure 4. Canonical correlation analysis (CCA) based on the relative abundances of operational taxonomic units (OTUs) and environmental factors. Shadow represents a significant difference in the prokaryotic community structure between the eddy core and edge at the same depth ($P < 0.05$, ANOSIM). Blue arrow is the environmental variable. Asterisks indicate the environmental factors that significantly influence the prokaryotic community structure using the envfit function (permutations = 999) (**$P < 0.01$, ***$P < 0.001$).

prokaryotic community structure exhibited significant differences between the eddy core and edge at 80, 100, and 120 m ($P < 0.05$; Figure 4). The community structure in the eddy core at these depths resembled more that of deeper depths than the community structure in the eddy edge at the same depth. Among the environmental factors, temperature exerted the most significant impact on the prokaryotic community structure (envfit analysis, $R^2 = 0.91$, $P < 0.001$), followed by salinity (envfit analysis, $R^2 = 0.87$, $P < 0.001$; Figure 4).

3.5. Differences in Enriched Taxa Between the Eddy Core and Edge

To identify the specific taxa contributing to increased HPP between 100 and 200 m in the eddy edge, genera-level taxa with a relative abundance exceeding 0.01% (coined "abundant taxa" in this study) were selected for comparing their relative abundances at 20–80 m, 100–200 m, and 300–500 m between the eddy core and edge using the LEfSe method (Figure 5). The results revealed a significant enrichment of the autotrophs *Prochlorococcus* and *Nitrosopumilus* (ammonia-oxidizing archaea), as well as the heterotrophic bacteria HTCC2188 (within the OM182 clade) and Arctic95A_2 (within the SAR406 clade), at 20–80 m in the eddy core (Figure 5). Most members of SAR406 are classified under the HNA group according to the literature (Table S2 in Supporting Information S1). However, nitrogen-fixing cyanobacteria UCYN-B and heterotrophic bacteria *Thalassobius* (Rhodobacterales), SAR86, and *Coraliomargarita* (Verrucomicrobia) were significantly enriched at 20–80 m in the eddy edge (Figure 5). Members of Rhodobacterales and SAR86 can be classified under the HNA and LNA groups, respectively, based on information from the literature (Table S2 in Supporting Information S1) and their genome size (Figure S6 in Supporting Information S1). At 100–200 m, the autotrophic nitrite-oxidizing bacteria *Nitrospina* exhibited a significant enrichment in the eddy core, while the heterotrophic SAR11 and HTCC2207 (within the SAR92 clade) were notably enriched in the eddy edge (Figure 5). SAR11 is classified under the LNA group based on information from the literature (Table S2 in Supporting Information S1) and its genome size (Figure S6 in Supporting Information S1). At 300–500 m, the heterotrophic bacteria *Owenweeksia* (Bacteroidetes) and MSBL3 (Verrucomicrobia) were notably enriched in the eddy core, while *Oleibacter* (Gammaproteobacteria) showed an enrichment in the eddy edge (Figure 5). Members of Bacteroidetes can be classified under the HNA group based on information from the literature (Table S2 in Supporting Information S1) and their genome size (Figure S6 in Supporting Information S1).

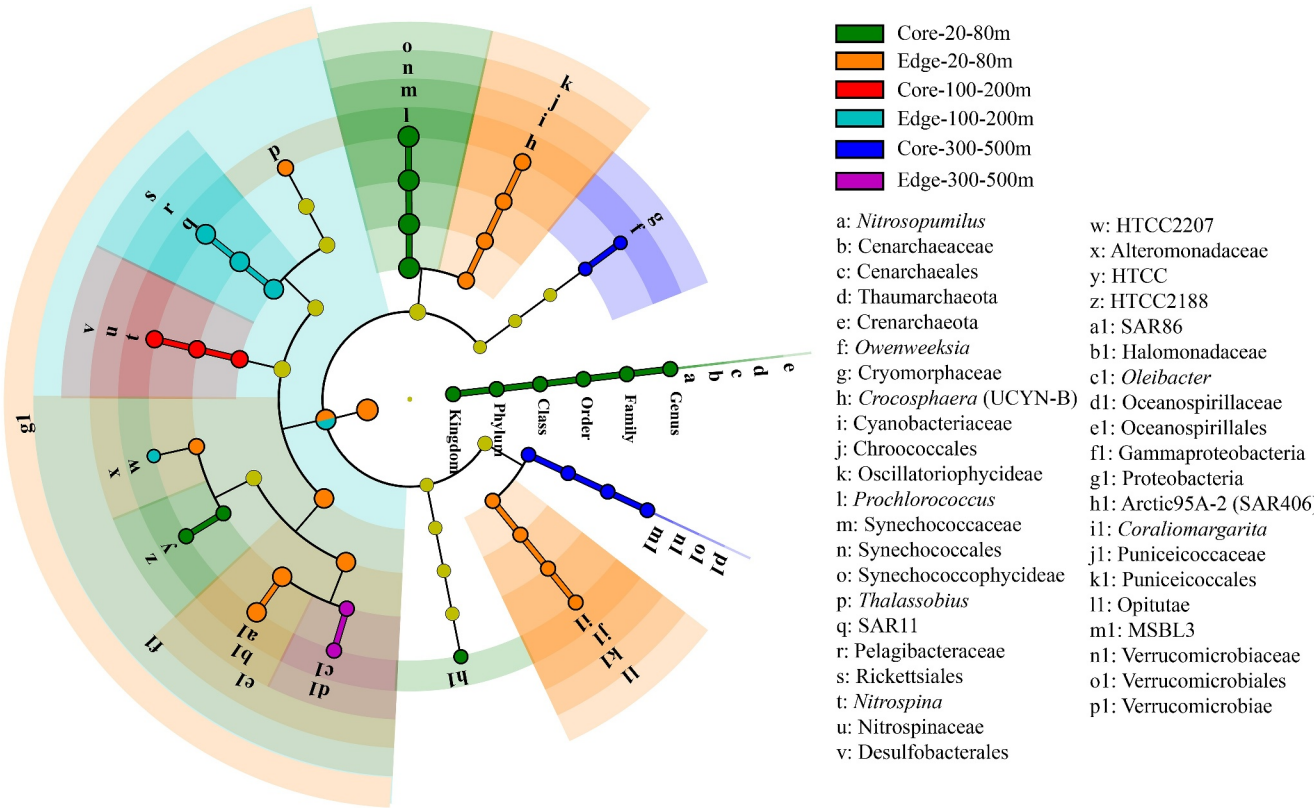

Figure 5. Enrichment analysis of genera-level taxa with an average relative abundance >0.01% between the eddy core and edge. The circles radiating from inside to outside designate the taxonomic levels from phylum to genus. Each small circle represents a taxon at the corresponding taxonomic level. The size of each small circle is proportional to the relative abundance of each taxon. The colors of circles indicate the zones where these taxa are significantly enriched [linear discriminant analysis (LDA) score >2, $P < 0.05$]. Yellowish-green circles indicate taxa that have no significant enrichment between the eddy core and edge (LDA score <2, $P > 0.05$).

3.6. Relationship Between Abundant Taxa and HPP

Spearman correlation analysis was conducted between the relative abundance of "abundant taxa" and total HPP, HNA%, and LNA%. Figure 6 showed a total of 32 taxa that had a significant relationship with HPP, with 15 taxa showing a positive correlation and 17 taxa showing a negative correlation ($P < 0.05$). Among these taxa, five were positively correlated with HNA% ($P < 0.05$), but negatively correlated with HPP, including MB11C04 (Puniceicoccaceae), Arctic95A-2, SargSea-WGS, as well as autotrophic *Nitrosopumilus* and *Nitrospina* (Figure 6). Arctic95A-2 and SargSea-WGS belong to the SAR406 clade. Among all 32 taxa, six were positively correlated with LNA% ($P < 0.05$), which included SAR11, ZA3312c, *Thalassobius*, *Coxiella*, as well as the autotrophic *Prochlorococcus* and *Synechococcus*, coincidentally showing a positive correlation with HPP (Figure 6). ZA3312c belongs to SAR406 and *Thalassobius* belongs to Rhodobacterales. Most members of SAR406 and Rhodobacterales are classified under the HNA group (Table S2 in Supporting Information S1), while SAR11 is categorized under the LNA group (Table S2 and Figure S6 in Supporting Information S1). SAR86 is also a typical member of the LNA group (Table S2 and Figure S6 in Supporting Information S1). While SAR86 did not exhibit a significantly positive correlation with LNA%, its relative abundance showed a positive correlation with HPP (Figure 6). In addition, *Formosa* (Bacteroidetes), *Maricaulis* (Rhodobacterales), HTCC2207 (Alteromonadales), *Nisaea* (Rhodospirillales), and members of Verrucomicrobia, despite not correlating with LNA%, were also found to be positively correlated with HPP (Figure 6).

4. Discussion

4.1. Stimulated Growth of Picophytoplankton in the Cyclonic Eddy Core and Enhanced HPP at the Edge

Nutrient upwelling in the core of the cyclonic eddy typically stimulates phytoplankton growth, resulting in an elevated concentration of chlorophyll at the eddy core, as evidenced by this study and previous research (Liu

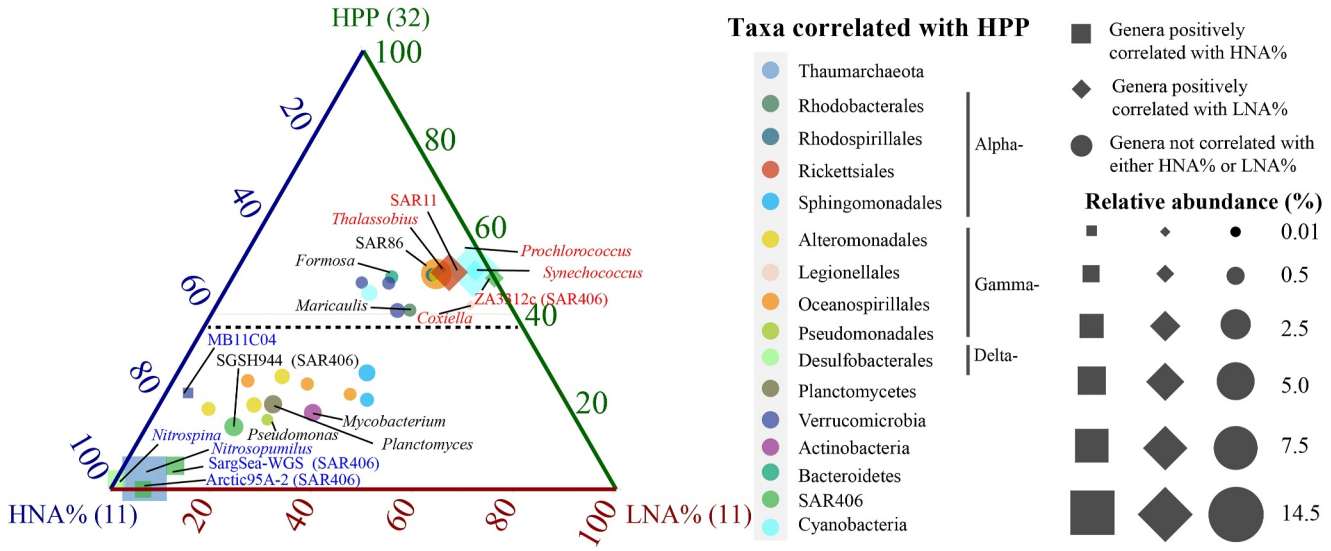

Figure 6. Ternary plot showing the relationships between the relative abundance of genera-level taxa (average relative abundance >0.01%) and heterotrophic prokaryotic production (HPP), as well as the proportions of HNA group (HNA%) and LNA group (LNA%) in total heterotrophic prokaryotic abundance for the upper 500 m ($P < 0.05$, Spearman). The correlation coefficient was normalized using Min-Max normalization for plotting, and the *P*-values were corrected by the Benjamini-Hochberg method. All genera (a total of 32) significantly correlated with HPP are shown, with 11 genera showing significant correlation with HNA% and LNA%. Genera above and below the black dashed line are significantly positively and negatively correlated with HPP, respectively. Each symbol represents one genus. Squares indicate a total of 5 genera that are significantly positively correlated with HNA% and negatively correlated with LNA% ($P < 0.05$, Spearman). Rhombuses indicate a total of 6 genera that are significantly positively correlated with LNA% and negatively correlated with HNA% ($P < 0.05$, Spearman). Circles indicate genera that are not significantly correlated with either HNA% or LNA%. The size of each symbol represents its average relative abundance, and the position of each symbol is determined by the proportion of the normalized correlation coefficient to the total sum.

et al., 2023; Rii et al., 2008; Wang et al., 2016). In the regions with high nutrient levels, such as near the Hawaiian island chain of subtropical northeastern Pacific, where the total inorganic nitrogen integrated above 150 m was almost seven times higher than in our study, there was an increased abundance of large-size (>3 μm) photosynthetic eukaryotes in a cyclonic eddy core, while *Synechococcus* and picoeukaryotes did not show an increase (Vaillancourt et al., 2003). However, in the extremely oligotrophic environment, such as the wNPSG we studied, picophytoplankton dominate with a competitive advantage over larger phytoplankton due to their higher nutrient affinity (Raven, 1998). Therefore, we observed a significant response of picophytoplankton to the cyclonic eddy of the wNPSG.

In the enriched picophytoplankton community, with the rise in NO_3^- concentration at the eddy core, the euphotic zone-integrated abundance of picoeukaryotes, *Synechococcus*, and *Prochlorococcus* was respectively 68.3 ± 0.7%, 44.6 ± 0.9%, and 24.0 ± 0.5% [$(mean_{core}\text{-}mean_{edge})/mean_{edge}$ ± propagated error] higher in the eddy core compared to the edge. The *Synechococcus* biomass showed the strongest linear correlation with NO_3^- concentration, suggesting that *Synechococcus* may have a greater capacity to utilize nitrate for growth than *Prochlorococcus* and picoeukaryotes in the cyclonic eddy. Similar findings were reported in the South China Sea where the abundance of *Synechococcus* and picoeukaryotes increased at a cyclonic eddy core compared to areas with lower nutrient levels, while no difference was observed in *Prochlorococcus* abundance between the eddy core and surrounding areas. Additionally, *Synechococcus* exhibited the strongest correlation with the nitracline depth (Chen et al., 2007). Utilizing a combination of nanoSIMS technology with ^{15}N-stable isotope labeling method, a study in the northwestern Atlantic has revealed the highest uptake rate of NO_3^- by *Synechococcus*, followed by pico-eukaryotes, and then *Prochlorococcus* (Berthelot et al., 2021). This is also consistent with the observation that *Prochlorococcus* was more abundant in warmer seawater with lower nitrate fluxes, while *Synechococcus* and picoeukaryotes were more abundant in colder seawater with higher nitrate fluxes in the Atlantic (Otero-Ferrer et al., 2018). While the streamlined genome of *Prochlorococcus* offers selective advantages in highly stable oligotrophic systems, it may limit their competitive edge in dynamic mixed regions (Bouman et al., 2011). This may partly explain why there is no significant increase of *Prochlorococcus* abundance in the eddy core compared to the edge.

The enhanced growth of phytoplankton could result in the release of more DOC, which may be utilized by heterotrophic prokaryotes, consequently boosting HPP in the cyclonic eddy. A previous study in the Eastern Tropical North Atlantic has shown high levels of chlorophyll *a*, primary production, DOC, and HPP at the periphery of the cyclonic eddy (Devresse et al., 2022). Similar patterns have also been observed in the southeastern Mediterranean, where the increased nutrients and primary production supported higher levels of heterotrophic prokaryotic metabolism in the cyclonic eddy compared to the anticyclonic eddy and reference station (Belkin et al., 2022). However, in our investigation in the wNPSG, despite the eddy core showing higher average chlorophyll fluorescence values and picophytoplankton abundances, the average HPP integrated above 500 m was 18.9 ± 1.0% higher at the eddy edge than the core. Especially, the significantly higher HPP was observed at 100–200 m in the eddy edge compared to the core ($P < 0.01$; Figure 3f). This observation suggests that factors other than phytoplankton may regulate the HPP (discussed in Section 4.3). Similar to our study, the spatial distribution of high HPP and chlorophyll concentration has been observed to decouple in the cyclonic eddy of the Southern Ocean (Fourquez et al., 2021).

4.2. Dominance of LNA Groups in HPP

The distribution pattern of LNA group abundance between the eddy core and edge more closely mirrored that of HPP compared to the HNA group (Figures 3b, 3c, and 3f). The Spearman correlation analysis showed that HPP has a much higher positive correlation coefficient with LNA group abundance compared to HNA ($P < 0.05$–0.001; Figure 7a and Figure S7 in Supporting Information S1). Furthermore, HPP was positively correlated with LNA% and negatively correlated with HNA% ($P < 0.05$–0.01; Figure 7a and Figure S7 in Supporting Information S1). These results suggest that the LNA group may be the primary contributors to HPP in the cyclonic eddy of the wNPSG, challenging the notion that the LNA group is inactive in aquatic systems (Lebaron et al., 2001). Consistent with our findings, a previous study in the coastal upwelling of Oregon found that the cell-specific leucine incorporation rates between the HNA and LNA groups showed no significant difference, indicating that the LNA group could be a crucial contributor to marine heterotrophic prokaryotic metabolism (Longnecker et al., 2005). Similarly, a previous study in the Southern Ocean demonstrated that cell-specific HPP peaked at the eddy core, where the LNA group accounted for approximately 95% of the heterotrophic prokaryote abundance, while they comprised less than 50% at the eddy edge (Fourquez et al., 2021). These literature findings support our conclusion that the LNA group can play a dominant role in contributing to HPP in the cyclonic eddy of the wNPSG.

Among the four heterotrophic taxa positively correlated with both HPP and LNA%—SAR11, ZA3312c, *Thalassobius*, and *Coxiella* (Figure 6) —SAR11 was the most abundant and identified as the typical LNA group (Fuchs et al., 2005; Mary et al., 2006; Schattenhofer et al., 2011; Vila-Costa et al., 2012) with a genome size ranging from 1.2 to 1.5 Mb (Figure S6 in Supporting Information S1). In line with the distribution of HPP, SAR11 was significantly enriched at the eddy edge, with a relative abundance reaching up to 15.4%, compared to the core within the depth range of 100–200 m (Figure 5). Therefore, we speculate that SAR11 may make a significant contribution to the observed higher HPP at the eddy edge compared to the core at 100–200 m depth. SAR11 has also been identified as a significant contributor to HPP, accounting for approximately 30%–50% of it in the Northwest Atlantic Ocean (Malmstrom et al., 2005). SAR86 was the second most abundant taxon that positively correlated with HPP and was also identified as a typical member of the LNA group (Zubkov et al., 2001). It is likely that SAR86 also significantly contributed to the HPP at the edge of the eddy since it has been reported to play a central role in the heterotrophic metabolism of organic carbon (Hoarfrost et al., 2020).

In addition, although most members of SAR406 and Rhodobacterales were thought to be the HNA group in the literature, some of members should still fall under the LNA category (Fuchs et al., 2005; Vila-Costa et al., 2012); for instance, known members of Rhodobacterales have a genome size range of 2.5–7.7 Mb, with some falling within the LNA range (Figure S6 and Table S2 in Supporting Information S1). Currently, SAR406 lacks a strain genome and a high-quality metagenome-assembled genome (MAG) for assessing its genome size. In uncultured SAR406, while two taxa displayed significant positive correlations with HNA% but negative correlations with HPP, ZA3312c exhibited significant positive correlations with both LNA% and HPP (Figure 6), suggesting that ZA3312c may contribute to this process as part of the LNA group. Similarly, *Coxiella* within Gammaproteobacteria currently lacks a marine strain genome or a high-quality MAG, whereas the non-marine strain of *Coxiella* has a genome size ranging from 0.6 to 2.2 Mb (Hammerl et al., 2015; Santos-Garcia et al., 2023). It is possible that

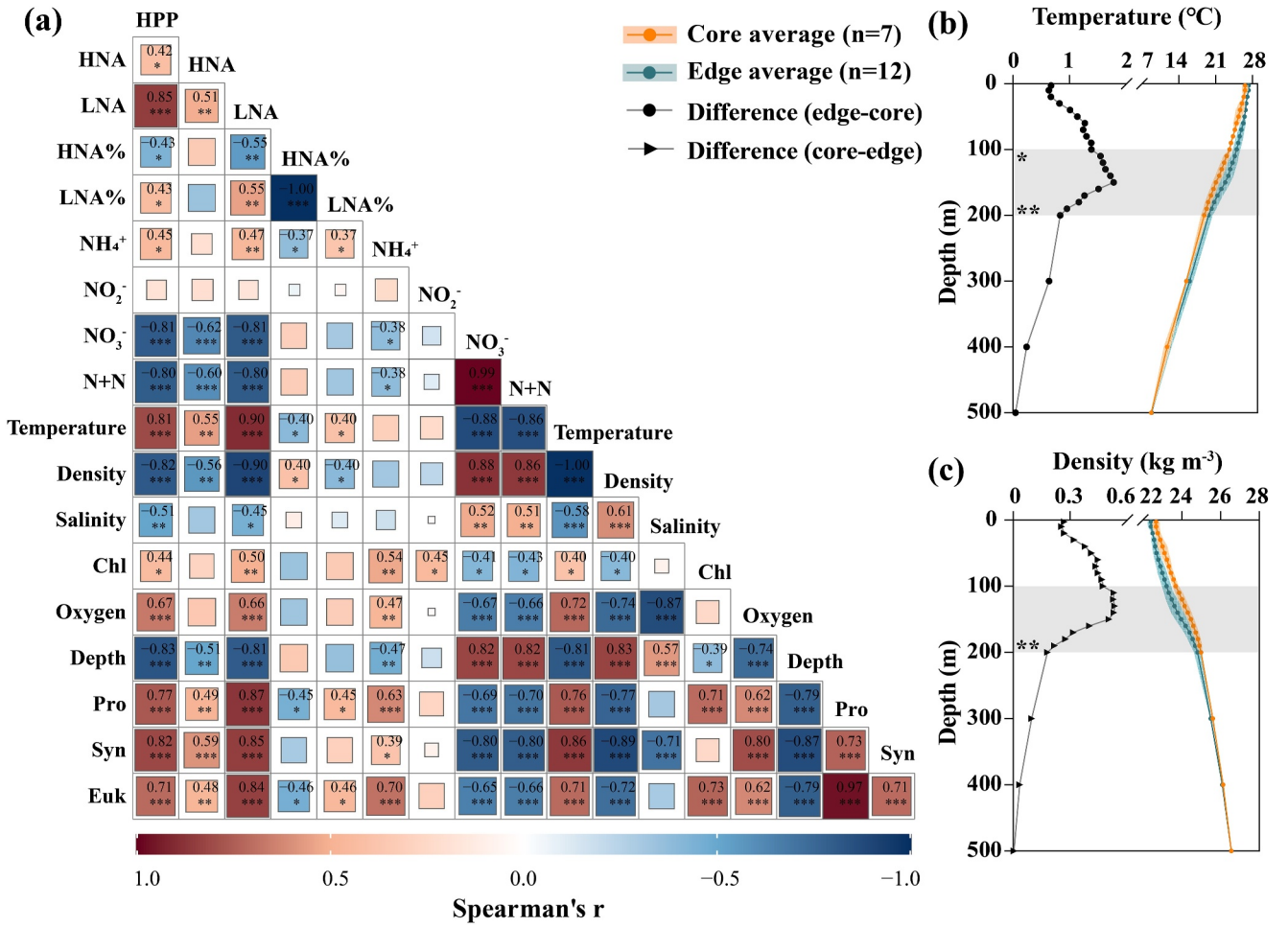

Figure 7. Spearman correlation analysis among biogeochemical parameters, and depth distributions of temperature and density. (a) Spearman correlations among biogeochemical parameters within 100–200 m ($n = 35$, $^{*}P < 0.05$, $^{**}P < 0.01$, $^{***}P < 0.001$). The *P*-values were corrected by the Benjamini-Hochberg method. HPP, heterotrophic prokaryotic production; HNA, high nucleic acid group; LNA, low nucleic acid group; HNA%, proportion of HNA group in total heterotrophic prokaryotic abundance; LNA%, proportion of LNA group in total heterotrophic prokaryotic abundance; NH_4^+, ammonium; NO_2^-, nitrite; NO_3^-, nitrate; N + N, sum of NO_2^- and NO_3^- concentrations; Chl, chlorophyll fluorescence; Pro, *Prochlorococcus*; Syn, *Synechococcus*; Euk, picoeukaryotes. (b) Depth profiles of average temperature and the temperature difference between the cyclonic edge and core. (c) Depth profiles of average density and the density difference between the cyclonic core and edge. The shaded area denotes the standard deviation (SD). Gray background indicates that the temperature and density difference within the 100–200 m was significantly greater than that above 100 m ($^{*}P < 0.05$) and 200–500 m ($^{**}P < 0.01$) using the Mann-Whitney *U* test, respectively.

Coxiella may also have a small genome in the ocean, belonging to the LNA group, and be active in HPP. Further research is warranted to clarify the specific contributions of HNA and LNA components to HPP.

4.3. Factors Inducing Higher HPP in the Cyclonic Eddy Edge

The upwelling in the cyclonic eddy core carries cold seawater from depth to the warmer euphotic zone, leading to changes in the temperature of the euphotic zone (Mikaelyan et al., 2023). In this study, the average temperature in the eddy core was consistently lower and the density higher than at the eddy edge throughout depths above 500 m ($P < 0.001$, Wilcoxon signed rank test), with the most pronounced contrast occurring between 100 and 200 m (Figures 7b and 7c). A previous study in the Western Pacific has established a significant positive correlation between HPP and ocean temperature (Rowe et al., 2012). Furthermore, a study collecting data on HPP in open oceans from the literature found that for every 1°C increase in seawater temperature above 200 m depth, HPP increased by 5% (Lønborg et al., 2016). Therefore, fluctuations in temperature may influence the variability of HPP within the cyclonic eddy. Consistent with the temperature distribution, we found that only LNA group abundance and HPP were significantly greater at the eddy edge than in the core at 100–200 m ($P < 0.05$–0.01, Mann-Whitney *U* test; Figures 3b and 3f), while HPP did not differ significantly between the eddy core and edge

at other depths (Figures 3b and 3f). Therefore, we speculate that relatively higher temperatures in the eddy edge may influence the distribution and activity of LNA cells, which thrive in warmer conditions (Otero-Ferrer et al., 2018) and dominate the abundance of total heterotrophic prokaryotes (Figure 3e), consequently enhancing HPP. In contrast, the lower temperatures at the eddy core may suppress the activity of heterotrophic prokaryotes. The speculation aligns with a study that observed a 47% increase in the activity of leucine aminopeptidase (LAPase), a proteolytic enzyme, at the end of laboratory warming experiments with seawater from the Great Barrier Reef when the temperature was increased by 3°C compared to the control group (Baltar et al., 2017). LAPase activity typically reflects HPP, for example, showing a positive correlation between them in the Northern South China Sea (Shi et al., 2019). The Spearman correlation analysis further demonstrated that among all environmental factors, HPP ($R = 0.89$ at 20–500 m and 0.81 at 100–200 m), LNA group abundance ($R = 0.90$ for both), and HNA group abundance ($R = 0.81$ and 0.55, respectively) consistently exhibited the strongest positive correlations with temperature ($P < 0.01$–0.001; Figure S7 in Supporting Information S1 and Figure 7a). Moreover, the highest correlation coefficient between LNA group abundance and temperature indicates the greatest sensitivity of LNA to temperature.

In addition, the Spearman correlation analysis indicated that HPP ($R = -0.88$ at 20–500 m and -0.81 at 100–200 m), LNA group abundance ($R = -0.89$ and -0.81, respectively), and HNA group abundance ($R = -0.82$ and -0.62, respectively) consistently showed the strongest negative correlations with nitrate concentration, excluding depth and density ($P < 0.001$; Figure S7 in Supporting Information S1 and Figure 7a). This may be related to the dilution effect of deep seawater, characterized by high nitrate and low microbial abundance, during upwelling. Furthermore, the negative correlations of LNA group abundance with nitrate were stronger than those of the HNA group. These findings are consistent with previous studies that have demonstrated the LNA group's higher adaptability to warm temperatures and low nitrate fluxes, for instance, at the edge of the cyclonic eddies in the Atlantic Ocean (Hernández-Hernández et al., 2020; Otero-Ferrer et al., 2018). Similarly, in this study, HNA% was significantly enriched at the eddy core, characterized by cooler temperatures and higher nitrate fluxes, while LNA % was enriched at the eddy edge, with warmer temperatures and lower nitrate fluxes at depths above 500 m ($P < 0.01$; Figures 3d and 3e). Notably, in contrast to nitrate, HPP ($R = 0.45$) and LNA group abundance ($R = 0.47$) were significantly positively correlated with ammonium concentration at 100–200 m (Figure 7a). Previous research has indicated that ammonium is the most frequently stimulatory nutrient for HPP, often showing a significant positive correlation between ammonium uptake by heterotrophic bacteria and HPP, while nitrate uptake shows no significant relation (Kirchman & Wheeler, 1998; Torréton et al., 2000). Therefore, the higher HPP at the eddy edge between 100 and 200 m, compared to the core, may result from the contribution of the more abundant LNA group stimulated by warmer temperatures (Figure 7b) and higher ammonium concentrations (Liu et al., 2023).

In contrast to our study, a study in the Southern Ocean indicated that the proportion of the LNA group in total heterotrophic prokaryotes was higher at the eddy core with lower temperature compared to the edge. However, this result was attributed to the significant likelihood of zooplankton predation on the HNA group within the core of the cyclonic eddy (Fourquez et al., 2021), as the HNA group is preyed upon more often than the LNA group due to their larger cell size (Gonzalez et al., 1990; Hu et al., 2020). Another study conducted during our cruise has found that mesozooplankton (>0.2 mm) abundances were approximately twice as high at the eddy core stations compared to the edge, with copepods being the main component, contributing an average of 89% to the mesozooplankton community across all stations (Liu et al., 2024). However, copepods are rarely found to feed directly on bacteria (Vargas & González, 2004). Furthermore, in the wNPSG dominated by picophytoplankton (80%–95% of total chlorophyll *a*) rather than diatoms (no more than 9%; Liu et al., 2024), copepods may primarily feed on protozoa instead of diatoms (Sommer & Sommer, 2006). Therefore, we speculate that the increased predation on protozoa by copepods in the eddy core may enable the HNA group to evade predation by protozoa, resulting in higher abundances and proportions of the HNA group above 100 m in the eddy core compared to the edge. Nevertheless, the lower temperatures and ammonium concentrations at the eddy core may have suppressed the activity of HNA groups (as well as LNA groups), as discussed above, which did not lead to a clearly elevated HPP at the core compared to the edge (Figure 3f).

The distribution of HPP can also be influenced by dissolved and particulate organic carbon. Previous studies have indicated that organic carbon tends to accumulate in the frontal region of eddies, thereby stimulating the increase in the abundance of heterotrophic prokaryotes (Arístegui & Montero, 2005; Baltar et al., 2009). In this study, the upwelling in the cyclonic eddy core transports seawater with low DOC concentrations from depth to the euphotic

zone, primarily in the 100–200 m depth. However, the DOC concentration shows a conservative distribution overall along isopycnals within the eddy system (data not shown). While the LNA group exhibited higher abundance between 100 and 200 m at the eddy edge compared to the core, the HNA group, known for its heightened response to increases in organic carbon (Wetz & Wheeler, 2004), showed no significant difference in abundance between the eddy core and edge in this depth zone (Figure 3c). Above 100 m, the abundance of both HNA and LNA groups was significantly higher at the eddy core than at the edge ($P < 0.05$–0.01; Figures 3b and 3c), potentially influenced by organic carbon produced by phytoplankton such as more abundant *Prochlorococcus*, *Synechococcus*, and picoeukaryotes ($P < 0.01$; Figure 2). However, there was no significant difference in HPP between the core and edge above 100 m (Figure 3f). Therefore, we can conclude that the increased HPP at the eddy edge between 100 and 200 m in this study was not primarily due to the stimulation of organic carbon.

The cyclonic eddy can also alter the light conditions of seawater (Wang et al., 2023), thereby influencing HPP (Moran & Miller, 2007; Ruiz-González et al., 2012). We observed that the enhanced growth of phytoplankton in the eddy core indeed altered light intensity, resulting in an uplift of the euphotic zone in the eddy core (~144 m) compared to the edge (~160 m; Figure 2d). It has been reported that light can stimulate the growth of SAR11 and SAR86 within the LNA group, as they may contain proteorhodopsin (Munson-McGee et al., 2022; Sánchez et al., 2020), which aligns with the significant enrichment of SAR11 and SAR86 at the eddy edge in this study (Figure 5). As a result, light may influence the distribution of SAR11 and SAR86, which could significantly contribute to HPP and, consequently, influence the distribution of HPP in the cyclonic eddy of the wNPSG. On the other hand, light may inhibit prokaryotes that are originally adapted to the deep sea. The upwelling can transport prokaryotes of deep-sea species (Nelson et al., 2014), as demonstrated by our observation that the community structure within the eddy core was more similar to that within the edge at deeper depths (Figure 4). The microorganisms transported from environments with no light or twilight conditions into the euphotic zone may encounter damage from intense light. For instance, certain members of SAR406, predominantly within the HNA group, exhibit a preference for darkness (Schwalbach et al., 2005). In this study, we observed that deep-sea members of SAR406, including Arctic95A-2, SGSH944, and SargSea-WGS, had significantly higher relative abundances at the eddy core than at the edge between 20 and 300 m ($P < 0.05$; Figure S8 in Supporting Information S1), likely due to the upwelling of the eddy core. Consequently, these deep-sea groups may experience damage from heightened light exposure at the eddy core, resulting in reduced activity and lower HPP between 100 and 200 m.

5. Conclusions

By tracking a cyclonic eddy during its mature stage in the western North Pacific subtropical gyre, we investigated the impact of the cyclonic eddy on picophytoplankton distribution, prokaryotic community composition, and HPP. Our focus on the potential contribution of HNA and LNA components to variations in HPP addresses a relatively understudied aspect of eddy-related research. The results revealed a spatial decoupling wherein higher picophytoplankton abundances (and total chlorophyll fluorescence) were observed in the eddy core, while higher HPP was evident between 100 and 200 m at the eddy edge. The LNA group, primarily dominated by SAR11 and SAR86, may be responsible for the elevated HPP at the edge. The relatively higher temperature, ammonium concentration, and light intensity induced by the cyclonic eddy at its edge may favor the enrichment and growth of the LNA group due to their high adaptability to warm temperatures, stimulation by ammonium, and the presence of proteorhodopsin in some members. This, in turn, may resulted in higher HPP at the eddy edge compared to the core. This study helps us better understand how HPP responds to cyclonic eddies in the oligotrophic open ocean. Future research necessitates an analysis of the activity of HNA and LNA groups at the single-cell level to better understand their contributions to HPP dynamics within cyclonic eddies.

Data Availability Statement

Biogeochemical data presented in this study are available on the Science Data Bank (Ni & Zhang, 2024, https://www.scidb.cn/anonymous/YmVNemFh). Daily sea level anomaly (SLA) data was obtained from the Copernicus Climate Change Service Climate Data Store (2018) (https://doi.org/10.24381/cds.4c328c78). The raw data of prokaryotic 16S rRNA genes was submitted to the National Center for Biotechnology Information (NCBI) Sequence Read Archive (SRA) (2024) database (accession number PRJNA1112995).

Acknowledgments
We sincerely thank all crew members of R/V *TAN KAH KEE* for their assistance in sampling and Tao Huang for the onboard measurement of ammonium concentration. This study was supported by grants from the National Natural Science Foundation of China (42125603 and 92251303) and the National Key Research and Development Program of China (2023YFF0805002).

References

Albright, L. J. (1975). The influence of hydrostatic pressure upon biochemical activities of heterotrophic bacteria. *Canadian Journal of Microbiology*, *21*(9), 1406–1412. https://doi.org/10.1139/m75-210

Apprill, A., McNally, S., Parsons, R., & Weber, L. (2015). Minor revision to V4 region SSU rRNA 806R gene primer greatly increases detection of SAR11 bacterioplankton. *Aquatic Microbial Ecology*, *75*(2), 129–137. https://doi.org/10.3354/ame01753

Arístegui, J., & Montero, M. F. (2005). Temporal and spatial changes in plankton respiration and biomass in the Canary Islands region: The effect of mesoscale variability. *Journal of Marine Systems*, *54*(1–4), 65–82. https://doi.org/10.1016/j.jmarsys.2004.07.004

Baltar, F., Arístegui, J., Montero, M. F., Espino, M., Gasol, J. M., & Herndl, G. J. (2009). Mesoscale variability modulates seasonal changes in the trophic structure of nano- and picoplankton communities across the NW Africa-Canary Islands transition zone. *Progress in Oceanography*, *83*(1–4), 180–188. https://doi.org/10.1016/j.pocean.2009.07.016

Baltar, F., Morán, X. A. G., & Lønborg, C. (2017). Warming and organic matter sources impact the proportion of dissolved to total activities in marine extracellular enzymatic rates. *Biogeochemistry*, *133*(3), 307–316. https://doi.org/10.1007/s10533-017-0334-9

Belkin, N., Guy-Haim, T., Rubin-Blum, M., Lazar, A., Sisma-Ventura, G., Kiko, R., et al. (2022). Influence of cyclonic and anticyclonic eddies on plankton in the southeastern Mediterranean Sea during late summertime. *Ocean Science*, *18*(3), 693–715. https://doi.org/10.5194/os-18-693-2022

Bentkowski, P., Van Oosterhout, C., & Mock, T. (2015). A model of genome size evolution for prokaryotes in stable and fluctuating environments. *Genome Biology and Evolution*, *7*(8), 2344–2351. https://doi.org/10.1093/gbe/evv148

Berthelot, H., Duhamel, S., L'Helguen, S., Maguer, J., & Cassar, N. (2021). Inorganic and organic carbon and nitrogen uptake strategies of picoplankton groups in the northwestern Atlantic Ocean. *Limnology & Oceanography*, *66*(10), 3682–3696. https://doi.org/10.1002/lno.11909

Bouman, H. A., Ulloa, O., Barlow, R., Li, W. K., Platt, T., Zwirglmaier, K., et al. (2011). Water-column stratification governs the community structure of subtropical marine picophytoplankton. *Environmental Microbiology Reports*, *3*(4), 473–482. https://doi.org/10.1111/j.1758-2229.2011.00241.x

Brown, S. L., Landry, M. R., Selph, K. E., Jin Yang, E., Rii, Y. M., & Bidigare, R. R. (2008). Diatoms in the desert: Plankton community response to a mesoscale eddy in the subtropical North Pacific. *Deep Sea Research Part II: Topical Studies in Oceanography*, *55*(10–13), 1321–1333. https://doi.org/10.1016/j.dsr2.2008.02.012

Chelton, D. B., Schlax, M. G., & Samelson, R. M. (2011). Global observations of nonlinear mesoscale eddies. *Progress in Oceanography*, *91*(2), 167–216. https://doi.org/10.1016/j.pocean.2011.01.002

Chen, Y. L. L., Chen, H. Y., Lin, I. I., Lee, M. A., & Chang, J. (2007). Effects of cold eddy on phytoplankton production and assemblages in Luzon strait bordering the South China Sea. *Journal of Oceanography*, *63*(4), 671–683. https://doi.org/10.1007/s10872-007-0059-9

Cole, J. R., Wang, Q., Fish, J. A., Chai, B., McGarrell, D. M., Sun, Y., et al. (2014). Ribosomal Database Project: Data and tools for high throughput rRNA analysis. *Nucleic Acids Research*, *42*(D1), D633–D642. https://doi.org/10.1093/nar/gkt1244

Copernicus Climate Change Service Climate Data Store. (2018). Sea level gridded data from satellite observations for the global ocean from 1993 to present [Dataset]. *Copernicus Climate Change Service (C3S) Climate Data Store (CDS)*. https://doi.org/10.24381/cds.4c328c78

Cruz, B. N., & Neuer, S. (2019). Heterotrophic bacteria enhance the aggregation of the marine picocyanobacteria Prochlorococcus and Synechococcus. *Frontiers in Microbiology*, *10*, 1864. https://doi.org/10.3389/fmicb.2019.01864

Dai, M., Wang, L., Guo, X., Zhai, W., Li, Q., He, B., & Kao, S. J. (2008). Nitrification and inorganic nitrogen distribution in a large perturbed river/estuarine system: The Pearl River Estuary, China. *Biogeosciences*, *5*(5), 1227–1244. https://doi.org/10.5194/bg-5-1227-2008

DeSantis, T. Z., Hugenholtz, P., Larsen, N., Rojas, M., Brodie, E. L., Keller, K., et al. (2006). Greengenes, a chimera-checked 16S rRNA gene database and workbench compatible with ARB. *Applied and Environmental Microbiology*, *72*(7), 5069–5072. https://doi.org/10.1128/AEM.03006-05

Devresse, Q., Becker, K. W., Bendinger, A., Hahn, J., & Engel, A. (2022). Eddy-enhanced primary production sustains heterotrophic microbial activities in the Eastern Tropical North Atlantic. *Biogeosciences*, *19*(22), 5199–5219. https://doi.org/10.5194/bg-19-5199-2022

Dore, J. E., Letelier, R. M., Church, M. J., Lukas, R., & Karl, D. M. (2008). Summer phytoplankton blooms in the oligotrophic North Pacific Subtropical Gyre: Historical perspective and recent observations. *Progress in Oceanography*, *76*(1), 2–38. https://doi.org/10.1016/j.pocean.2007.10.002

Edgar, R. C. (2013). Highly accurate OTU sequences from microbial amplicon reads. *Nature Methods*, *10*(10), 996–998. https://doi.org/10.1038/nmeth.2604

Falkowski, P. G., Ziemann, D., Kolber, Z., & Bienfang, P. (1991). Role of eddy pumping in enhancing primary production in the ocean. *Nature*, *352*(6330), 55–58. https://doi.org/10.1038/352055a0

Fourquez, M., Strzepek, R., Ellwood, M. J., Hassler, C., Cabanes, D., Eggins, S., et al. (2021). Response of Subantarctic microbes to new versus regenerated Fe in a cold-core eddy. *Authorea Preprints*. https://doi.org/10.1002/essoar.10509393.1

Fuchs, B., Woebken, D., Zubkov, M., Burkill, P., & Amann, R. (2005). Molecular identification of picoplankton populations in contrasting waters of the Arabian Sea. *Aquatic Microbial Ecology*, *39*, 145–157. https://doi.org/10.3354/ame039145

Gasol, J. M., Vázquez-Domínguez, E., Vaqué, D., Agustí, S., & Duarte, C. M. (2009). Bacterial activity and diffusive nutrient supply in the oligotrophic Central Atlantic Ocean. *Aquatic Microbial Ecology*, *56*(1), 1–12. https://doi.org/10.3354/ame01310

Gasol, J. M., Zweifel, U. L., Peters, F., Fuhrman, J. A., & Hagström, Å. (1999). Significance of size and nucleic acid content heterogeneity as measured by flow cytometry in natural planktonic bacteria. *Applied and Environmental Microbiology*, *65*(10), 4475–4483. https://doi.org/10.1128/AEM.65.10.4475-4483.1999

Giovannoni, S. J. (2017). SAR11 bacteria: The most abundant plankton in the oceans. *Annual Review of Marine Science*, *9*(1), 231–255. https://doi.org/10.1146/annurev-marine-010814-015934

Giovannoni, S. J., Tripp, H. J., Givan, S., Podar, M., Vergin, K. L., Baptista, D., et al. (2005). Genome streamlining in a cosmopolitan oceanic bacterium. *Science*, *309*(5738), 1242–1245. https://doi.org/10.1126/science.1114057

Gonzalez, J. M., Sherr, E. B., & Sherr, B. F. (1990). Size-selective grazing on bacteria by natural assemblages of estuarine flagellates and ciliates. *Applied and Environmental Microbiology*, *56*(3), 583–589. https://doi.org/10.1128/aem.56.3.583-589.1990

Hammerl, J. A., Mertens, K., Sprague, L. D., Hackert, V. H., Buijs, J., Hoebe, C. J., et al. (2015). First draft genome sequence of a human Coxiella burnetii isolate, originating from the largest Q fever outbreak ever reported, The Netherlands, 2007 to 2010. *Genome Announcements*, *3*(3), 00445515. https://doi.org/10.1128/genomeA.00445-15

Hernández-Hernández, N., Arístegui, J., Montero, M. F., Velasco-Senovilla, E., Baltar, F., Marrero-Díaz, Á., et al. (2020). Drivers of plankton distribution across mesoscale eddies at submesoscale range. *Frontiers in Marine Science*, *7*, 667. https://doi.org/10.3389/fmars.2020.00667

Hoarfrost, A., Nayfach, S., Ladau, J., Yooseph, S., Arnosti, C., Dupont, C. L., & Pollard, K. S. (2020). Global ecotypes in the ubiquitous marine clade SAR86. *The ISME Journal*, *14*(1), 178–188. https://doi.org/10.1038/s41396-019-0516-7

Hu, C., Chen, X., Yu, L., Xu, D., & Jiao, N. (2020). Elevated contribution of low nucleic acid prokaryotes and viral lysis to the prokaryotic community along the nutrient gradient from an estuary to open ocean transect. *Frontiers in Microbiology*, *11*, 612053. https://doi.org/10.3389/fmicb.2020.612053

Hu, Z., Tan, Y., Song, X., Zhou, L., Lian, X., Huang, L., & He, Y. (2014). Influence of mesoscale eddies on primary production in the South China Sea during spring inter-monsoon period. *Acta Oceanologica Sinica*, *33*(3), 118–128. https://doi.org/10.1007/s13131-014-0431-8

Huang, Y., Chen, B., Huang, B., Zhou, H., & Yuan, Y. (2019). Potential overestimation of community respiration in the western Pacific boundary ocean: What causes the putative net heterotrophy in oligotrophic systems? *Limnology & Oceanography*, *64*(5), 2202–2219. https://doi.org/10.1002/lno.11179

Karl, D. M. (1999). A sea of change: Biogeochemical variability in the North Pacific Subtropical Gyre. *Ecosystems*, *2*(3), 181–214. https://doi.org/10.1007/s100219900068

Kirchman, D., K'nees, E., & Hodson, R. (1985). Leucine incorporation and its potential as a measure of protein synthesis by bacteria in natural aquatic systems. *Applied and Environmental Microbiology*, *49*(3), 599–607. https://doi.org/10.1128/aem.49.3.599-607.1985

Kirchman, D. L., & Wheeler, P. A. (1998). Uptake of ammonium and nitrate by heterotrophic bacteria and phytoplankton in the sub-Arctic Pacific. *Deep Sea Research Part I: Oceanographic Research Papers*, *45*(2–3), 347–365. https://doi.org/10.1016/S0967-0637(97)00075-7

Lebaron, P., Servais, P., Agogué, H., Courties, C., & Joux, F. (2001). Does the high nucleic acid content of individual bacterial cells allow us to discriminate between active cells and inactive cells in aquatic systems? *Applied and Environmental Microbiology*, *67*(4), 1775–1782. https://doi.org/10.1128/AEM.67.4.1775-1782.2001

Li, B., Karl, D., Letelier, R., & Church, M. (2011). Size-dependent photosynthetic variability in the North Pacific Subtropical Gyre. *Marine Ecology Progress Series*, *440*, 27–40. https://doi.org/10.3354/meps09345

Liu, H., Browning, T. J., Laws, E. A., Huang, Y., Wang, L., Shang, Y., et al. (2024). Stimulation of small phytoplankton drives enhanced sinking particle formation in a subtropical ocean eddy. *Limnology & Oceanography*, *69*(4), 834–847. https://doi.org/10.1002/lno.12529

Liu, L., Chen, M., Wan, X. S., Du, C., Liu, Z., Hu, Z., et al. (2023). Reduced nitrite accumulation at the primary nitrite maximum in the cyclonic eddies in the western North Pacific subtropical gyre. *Science Advances*, *9*(33), eade2078. https://doi.org/10.1126/sciadv.ade2078

Lønborg, C., Cuevas, L. A., Reinthaler, T., Herndl, G. J., Gasol, J. M., Morán, X. A. G., et al. (2016). Depth dependent relationships between temperature and ocean heterotrophic prokaryotic production. *Frontiers in Marine Science*, *3*, 90. https://doi.org/10.3389/fmars.2016.00090

Longnecker, K., Sherr, B. F., & Sherr, E. B. (2005). Activity and phylogenetic diversity of bacterial cells with high and low nucleic acid content and electron transport system activity in an upwelling ecosystem. *Applied and Environmental Microbiology*, *71*(12), 7737–7749. https://doi.org/10.1128/AEM.71.12.7737-7749.2005

Magoč, T., & Salzberg, S. L. (2011). FLASH: Fast length adjustment of short reads to improve genome assemblies. *Bioinformatics*, *27*(21), 2957–2963. https://doi.org/10.1093/bioinformatics/btr507

Malmstrom, R. R., Cottrell, M. T., Elifantz, H., & Kirchman, D. L. (2005). Biomass production and assimilation of dissolved organic matter by SAR11 bacteria in the Northwest Atlantic Ocean. *Applied and Environmental Microbiology*, *71*(6), 2979–2986. https://doi.org/10.1128/AEM.71.6.2979-2986.2005

Marie, D., Partensky, F., Jacquet, S., & Vaulot, D. (1997). Enumeration and cell cycle analysis of natural populations of marine picoplankton by flow cytometry using the nucleic acid stain SYBR Green I. *Applied and Environmental Microbiology*, *63*(1), 186–193. https://doi.org/10.1128/aem.63.1.186-193.1997

Mary, I., Heywood, J. L., Fuchs, B. M., Amann, R., Tarran, G. A., Burkill, P. H., & Zubkov, M. V. (2006). SAR11 dominance among metabolically active low nucleic acid bacterioplankton in surface waters along an Atlantic meridional transect. *Aquatic Microbial Ecology*, *45*, 107–113. https://doi.org/10.3354/ame045107

McDonald, D., Price, M. N., Goodrich, J., Nawrocki, E. P., DeSantis, T. Z., Probst, A., et al. (2012). An improved Greengenes taxonomy with explicit ranks for ecological and evolutionary analyses of bacteria and archaea. *The ISME Journal*, *6*(3), 610–618. https://doi.org/10.1038/ismej.2011.139

Mikaelyan, A. S., Zatsepin, A. G., Kubryakov, A. A., Podymov, O. I., Mosharov, S. A., Pautova, L. A., et al. (2023). Case where a mesoscale cyclonic eddy suppresses primary production: A Stratification-Lock hypothesis. *Progress in Oceanography*, *212*, 102984. https://doi.org/10.1016/j.pocean.2023.102984

Mojica, K. D., Carlson, C. A., & Behrenfeld, M. J. (2020). Regulation of low and high nucleic acid fluorescent heterotrophic prokaryote subpopulations and links to viral-induced mortality within natural prokaryote-virus communities. *Microbial Ecology*, *79*(1), 213–230. https://doi.org/10.1007/s00248-019-01393-9

Moran, M. A., & Miller, W. L. (2007). Resourceful heterotrophs make the most of light in the coastal ocean. *Nature Reviews Microbiology*, *5*(10), 792–800. https://doi.org/10.1038/nrmicro1746

Munson-McGee, J. H., Lindsay, M. R., Sintes, E., Brown, J. M., D'Angelo, T., Brown, J., et al. (2022). Decoupling of respiration rates and abundance in marine prokaryoplankton. *Nature*, *612*(7941), 764–770. https://doi.org/10.1038/s41586-022-05505-3

Nagata, T., Fukuda, H., Fukuda, R., & Koike, I. (2000). Bacterioplankton distribution and production in deep Pacific waters: Large–scale geographic variations and possible coupling with sinking particle fluxes. *Limnology & Oceanography*, *45*(2), 426–435. https://doi.org/10.4319/lo.2000.45.2.0426

National Center for Biotechnology Information (NCBI) Sequence Read Archive (SRA). (2024). Elevated heterotrophic prokaryotic production supported by low nucleic acid prokaryotes at a cyclonic eddy edge in the Northwest Pacific [Dataset]. *NCBI*. https://www.ncbi.nlm.nih.gov/sra/PRJNA1112995

Nelson, C. E., Carlson, C. A., Ewart, C. S., & Halewood, E. R. (2014). Community differentiation and population enrichment of Sargasso Sea bacterioplankton in the euphotic zone of a mesoscale mode-water eddy. *Environmental Microbiology*, *16*(3), 871–887. https://doi.org/10.1111/1462-2920.12241

Ni, J., & Zhang, Y. (2024). Biogeochemical dataset for 'Elevated heterotrophic prokaryotic production supported by low nucleic acid prokaryotes at a cyclonic eddy edge in the Northwest Pacific' [Dataset]. *Science Data Bank*. https://www.scidb.cn/anonymous/YmVNemFh

Olson, R. J., Chisholm, S. W., Zettler, E. R., Altabet, M. A., & Dusenberry, J. A. (1990). Spatial and temporal distributions of prochlorophyte picoplankton in the North Atlantic Ocean. *Deep-Sea Research, Part A: Oceanographic Research Papers*, *37*(6), 1033–1051. https://doi.org/10.1016/0198-0149(90)90109-9

Otero-Ferrer, J. L., Cermeño, P., Bode, A., Fernández-Castro, B., Gasol, J. M., Morán, X. A. G., et al. (2018). Factors controlling the community structure of picoplankton in contrasting marine environments. *Biogeosciences*, *15*(20), 6199–6220. https://doi.org/10.5194/bg-15-6199-2018

Parada, A. E., Needham, D. M., & Fuhrman, J. A. (2016). Every base matters: Assessing small subunit rRNA primers for marine microbiomes with mock communities, time series and global field samples. *Environmental Microbiology*, *18*(5), 1403–1414. https://doi.org/10.1111/1462-2920.13023

Pomeroy, L. R., & Wiebe, W. J. (2001). Temperature and substrates as interactive limiting factors for marine heterotrophic bacteria. *Aquatic Microbial Ecology*, *23*, 187–204. https://doi.org/10.3354/ame023187

Qiu, B., Chen, S., Klein, P., Sasaki, H., & Sasai, Y. (2014). Seasonal mesoscale and submesoscale eddy variability along the North Pacific Subtropical Countercurrent. *Journal of Physical Oceanography*, *44*(12), 3079–3098. https://doi.org/10.1175/JPO-D-14-0071.1

Raven, J. A. (1998). The twelfth Tansley Lecture. Small is beautiful: The picophytoplankton: Picophyto-plankton. *Functional Ecology*, *12*(4), 503–513. https://doi.org/10.1046/j.1365-2435.1998.00233.x

Rii, Y. M., Brown, S. L., Nencioli, F., Kuwahara, V., Dickey, T., Karl, D. M., & Bidigare, R. R. (2008). The transient oasis: Nutrient-phytoplankton dynamics and particle export in Hawaiian lee cyclones. *Deep Sea Research Part II: Topical Studies in Oceanography*, *55*(10–13), 1275–1290. https://doi.org/10.1016/j.dsr2.2008.01.013

Rii, Y. M., Karl, D. M., & Church, M. J. (2016). Temporal and vertical variability in picophytoplankton primary productivity in the North Pacific Subtropical Gyre. *Marine Ecology Progress Series*, *562*, 1–18. https://doi.org/10.3354/meps11954

Robidart, J. C., Magasin, J. D., Shilova, I. N., Turk-Kubo, K. A., Wilson, S. T., Karl, D. M., et al. (2019). Effects of nutrient enrichment on surface microbial community gene expression in the oligotrophic North Pacific Subtropical Gyre. *The ISME Journal*, *13*(2), 374–387. https://doi.org/10.1038/s41396-018-0280-0

Rowe, J. M., DeBruyn, J. M., Poorvin, L., LeCleir, G. R., Johnson, Z. I., Zinser, E. R., & Wilhelm, S. W. (2012). Viral and bacterial abundance and production in the Western Pacific Ocean and the relation to other oceanic realms. *FEMS Microbiology Ecology*, *79*(2), 359–370. https://doi.org/10.1111/j.1574-6941.2011.01223.x

Ruiz-González, C., Galí, M., Lefort, T., Cardelús, C., Simó, R., & Gasol, J. M. (2012). Annual variability in light modulation of bacterial heterotrophic activity in surface northwestern Mediterranean waters. *Limnology & Oceanography*, *57*(5), 1376–1388. https://doi.org/10.4319/lo.2012.57.5.1376

Sánchez, O., Ferrera, I., Mabrito, I., Gazulla, C. R., Sebastián, M., Auladell, A., et al. (2020). Seasonal impact of grazing, viral mortality, resource availability and light on the group-specific growth rates of coastal Mediterranean bacterioplankton. *Scientific Reports*, *10*(1), 19773. https://doi.org/10.1038/s41598-020-76590-5

Santos-Garcia, D., Morel, O., Henri, H., El Filali, A., Buysse, M., Noël, V., et al. (2023). Genomic changes during the evolution of the Coxiella genus along the parasitism-mutualism continuum. *Peer Community Journal*, *3*, e41. https://doi.org/10.24072/pcjournal

Scharek, R., & Latasa, M. (2007). Growth, grazing and carbon flux of high and low nucleic acid bacteria differ in surface and deep chlorophyll maximum layers in the NW Mediterranean Sea. *Aquatic Microbial Ecology*, *46*, 153–161. https://doi.org/10.3354/ame046153

Schattenhofer, M., Wulf, J., Kostadinov, I., Glöckner, F. O., Zubkov, M. V., & Fuchs, B. M. (2011). Phylogenetic characterisation of picoplanktonic populations with high and low nucleic acid content in the North Atlantic Ocean. *Systematic & Applied Microbiology*, *34*(6), 470–475. https://doi.org/10.1016/j.syapm.2011.01.008

Schwalbach, M., Brown, M., & Fuhrman, J. (2005). Impact of light on marine bacterioplankton community structure. *Aquatic Microbial Ecology*, *39*, 235–245. https://doi.org/10.3354/ame039235

Shi, Z., Xu, J., Li, X., Li, R., & Li, Q. (2019). Links of extracellular enzyme activities, microbial metabolism, and community composition in the river-impacted coastal waters. *Journal of Geophysical Research: Biogeosciences*, *124*(11), 3507–3520. https://doi.org/10.1029/2019JG005095

Singh, A., Gandhi, N., Ramesh, R., & Prakash, S. (2015). Role of cyclonic eddy in enhancing primary and new production in the Bay of Bengal. *Journal of Sea Research*, *97*, 5–13. https://doi.org/10.1016/j.seares.2014.12.002

Sommer, U., & Sommer, F. (2006). Cladocerans versus copepods: The cause of contrasting top–down controls on freshwater and marine phytoplankton. *Oecologia*, *147*(2), 183–194. https://doi.org/10.1007/s00442-005-0320-0

Torréton, J. P., Talbot, V., & Garcia, N. (2000). Nutrient stimulation of bacterioplankton growth in Tuamotu atoll lagoons. *Aquatic Microbial Ecology*, *21*(2), 125–137. https://doi.org/10.3354/ame021125

Vaillancourt, R. D., Marra, J., Seki, M. P., Parsons, M. L., & Bidigare, R. R. (2003). Impact of a cyclonic eddy on phytoplankton community structure and photosynthetic competency in the subtropical North Pacific Ocean. *Deep Sea Research Part I: Oceanographic Research Papers*, *50*(7), 829–847. https://doi.org/10.1016/S0967-0637(03)00059-1

Van Wambeke, F., Catala, P., Pujo-Pay, M., & Lebaron, P. (2011). Vertical and longitudinal gradients in HNA-LNA cell abundances and cytometric characteristics in the Mediterranean Sea. *Biogeosciences*, *8*(7), 1853–1863. https://doi.org/10.5194/bg-8-1853-2011

Vargas, C. A., & González, H. E. (2004). Plankton community structure and carbon cycling in a coastal upwelling system. I. Bacteria, microprotozoans and phytoplankton in the diet of copepods and appendicularians. *Aquatic Microbial Ecology*, *34*(2), 151–164. https://doi.org/10.3354/ame034151

Vila-Costa, M., Gasol, J. M., Sharma, S., & Moran, M. A. (2012). Community analysis of high- and low-nucleic acid-containing bacteria in NW Mediterranean coastal waters using 16S rDNA pyrosequencing. *Environmental Microbiology*, *14*(6), 1390–1402. https://doi.org/10.1111/j.1462-2920.2012.02720.x

Vila-Costa, M., Sebastián, M., Pizarro, M., Cerro-Gálvez, E., Lundin, D., Gasol, J. M., & Dachs, J. (2019). Microbial consumption of organophosphate esters in seawater under phosphorus limited conditions. *Scientific Reports*, *9*(1), 233. https://doi.org/10.1038/s41598-018-36635-2

Wang, L., Huang, B., Chiang, K.-P., Liu, X., Chen, B., Xie, Y., et al. (2016). Physical-biological coupling in the western South China Sea: The response of phytoplankton community to a mesoscale cyclonic eddy. *PLoS One*, *11*(4), e0153735. https://doi.org/10.1371/journal.pone.0153735

Wang, Y., Yang, J., & Chen, G. (2023). Euphotic zone depth anomaly in global mesoscale eddies by multi-mission fusion data. *Remote Sensing*, *15*(4), 1062. https://doi.org/10.3390/rs15041062

Wei, Y., Zhang, Z., Cui, Z., & Sun, J. (2021). Size-fractionated biogenic silica standing stocks and carbon biomass in the western tropical North Pacific: Evidence for the ecological importance of pico-sized plankton in oligotrophic gyres. *Frontiers in Marine Science*, *8*, 691367. https://doi.org/10.3389/fmars.2021.691367

Wetz, M., & Wheeler, P. (2004). Response of bacteria to simulated upwelling phytoplankton blooms. *Marine Ecology Progress Series*, *272*, 49–57. https://doi.org/10.3354/meps272049

Zhang, J. Z. (2000). Shipboard automated determination of trace concentrations of nitrite and nitrate in oligotrophic water by gas-segmented continuous flow analysis with a liquid waveguide capillary flow cell. *Deep Sea Research Part I: Oceanographic Research Papers*, *47*(6), 1157–1171. https://doi.org/10.1016/S0967-0637(99)00085-0

Zhu, Y., Yuan, D., Huang, Y., Ma, J., & Feng, S. (2013). A sensitive flow-batch system for on board determination of ultra-trace ammonium in seawater: Method development and shipboard application. *Analytica Chimica Acta*, *794*, 47–54. https://doi.org/10.1016/j.aca.2013.08.009

Zubkov, M. V., Fuchs, B. M., Burkill, P. H., & Amann, R. (2001). Comparison of cellular and biomass specific activities of dominant bacterioplankton groups in stratified waters of the Celtic Sea. *Applied and Environmental Microbiology*, *67*(11), 5210–5218. https://doi.org/10.1128/AEM.67.11.5210-5218.2001

References From the Supporting Information

Campbell, L., Nolla, H., & Vaulot, D. (1994). The importance of Prochlorococcus to community structure in the central North Pacific Ocean. *Limnology & Oceanography*, *39*(4), 954–961. https://doi.org/10.4319/lo.1994.39.4.0954

Casey, J. R., Björkman, K. M., Ferrón, S., & Karl, D. M. (2019). Size dependence of metabolism within marine picoplankton populations. *Limnology & Oceanography*, *64*(4), 1819–1827. https://doi.org/10.1002/lno.11153

Chen, I.-M. A., Chu, K., Palaniappan, K., Pillay, M., Ratner, A., Huang, J., et al. (2019). IMG/M v. 5.0: An integrated data management and comparative analysis system for microbial genomes and microbiomes. *Nucleic Acids Research*, *47*(D1), D666–D677. https://doi.org/10.1093/nar/gky901

Connell, P. E., Ribalet, F., Armbrust, E. V., White, A., & Caron, D. A. (2020). Diel oscillations in the feeding activity of heterotrophic and mixotrophic nanoplankton in the North Pacific Subtropical Gyre. *Aquatic Microbial Ecology*, *85*, 167–181. https://doi.org/10.3354/ame01950

DuRand, M. D., Olson, R. J., & Chisholm, S. W. (2001). Phytoplankton population dynamics at the Bermuda Atlantic time-series station in the Sargasso sea. *Deep Sea Research Part II: Topical Studies in Oceanography*, *48*(8–9), 1983–2003. https://doi.org/10.1016/S0967-0645(00)00166-1

Garrison, D. L., Gowing, M. M., Hughes, M. P., Campbell, L., Caron, D. A., Dennett, M. R., et al. (2000). Microbial food web structure in the Arabian sea: A US JGOFS study. *Deep Sea Research Part II: Topical Studies in Oceanography*, *47*(7–8), 1387–1422. https://doi.org/10.1016/S0967-0645(99)00148-4

Kawasaki, N., Sohrin, R., Ogawa, H., Nagata, T., & Benner, R. (2011). Bacterial carbon content and the living and detrital bacterial contributions to suspended particulate organic carbon in the North Pacific Ocean. *Aquatic Microbial Ecology*, *62*(2), 165–176. https://doi.org/10.3354/ame01462

Lange, P. K., Brewin, R. J., Dall'Olmo, G., Tarran, G. A., Sathyendranath, S., Zubkov, M., & Bouman, H. A. (2018). Scratching beneath the surface: A model to predict the vertical distribution of Prochlorococcus using remote sensing. *Remote Sensing*, *10*(6), 847. https://doi.org/10.3390/rs10060847

Liu, H., Chang, J., Tseng, C.-M., Wen, L.-S., & Liu, K. (2007). Seasonal variability of picoplankton in the Northern South China Sea at the SEATS station. *Deep Sea Research Part II: Topical Studies in Oceanography*, *54*(14–15), 1602–1616. https://doi.org/10.1016/j.dsr2.2007.05.004

Tarran, G. A., Heywood, J. L., & Zubkov, M. V. (2006). Latitudinal changes in the standing stocks of nano- and picoeukaryotic phytoplankton in the Atlantic Ocean. *Deep Sea Research Part II: Topical Studies in Oceanography*, *53*(14–16), 1516–1529. https://doi.org/10.1016/j.dsr2.2006.05.004

Taylor, A. G., & Landry, M. R. (2018). Phytoplankton biomass and size structure across trophic gradients in the southern California Current and adjacent ocean ecosystems. *Marine Ecology Progress Series*, *592*, 1–17. https://doi.org/10.3354/meps12526

Wei, Y., Sun, J., Zhang, X., Wang, J., & Huang, K. (2019). Picophytoplankton size and biomass around equatorial eastern Indian Ocean. *Microbiologica*, *8*(2), e00629. https://doi.org/10.1002/mbo3.629

Worden, A. Z., Nolan, J. K., & Palenik, B. (2004). Assessing the dynamics and ecology of marine picophytoplankton: The importance of the eukaryotic component. *Limnology & Oceanography*, *49*(1), 168–179. https://doi.org/10.4319/lo.2004.49.1.0168